Title

PRELIMINARY ESTIMATION OF THE RESERVOIR CAPACITY AND THE LONGEVITY OF THE BACA GEOTHERMAL FIELD, NEW MEXICO

Permalink

https://escholarship.org/uc/item/6ff291zt

Authors

Bodvarsson, G.S.
Haar, S. Vonder
Wilt, M.
et al.

Publication Date

1980-07-01

CONF-800931--4

Presented at the 55th Annual Technical
Conference and Exhibition, Society of
Petroleum Engineers of the American
Institute of Mining, Metallurgical and
Petroleum Engineers, Inc., Dallas, TX
September 21-24, 1980

LBL-10656

MASTER

PRELIMINARY ESTIMATION OF THE RESERVOIR CAPACITY AND THE LONGEVITY OF THE BACA GEOTHERMAL FIELD, NEW MEXICO

G.S. Bodvarsson, S. Vonder Haar,
M. Wilt, and C.F. Tsang

July 1980

Prepared for the U.S. Department of Energy
under Contract W-7405-ENG-48

LAWRENCE BERKELEY LABORATORY
UNIVERSITY OF CALIFORNIA
BERKELEY

DISCLAIMER

LBL-10656

PRELIMINARY ESTIMATION OF THE RESERVOIR CAPACITY AND THE LONGEVITY OF THE BACA GEOTHERMAL FIELD, NEW MEXICO

G.S. Bodvarsson, S. Vonder Haar, M. Wilt and C.F. Tsang

ABSTRACT

A 50 MW geothermal power plant is currently under development at the Baca site in the Valles Caldera, New Mexico, as a joint venture of the Department of Energy (DOE), Union Oil Company of California and the Public Service Company of New Mexico (PNM). To date, over 20 wells have been drilled on the prospect, and the data from these wells indicate the presence of a high-temperature liquid dominated reservoir. In this paper, data from open literature on the field are used to estimate the amount of hot water in place (reservoir capacity) and the length of time the reservoir can supply steam for a 50 MW power plant (reservoir longevity).

The reservoir capacity is estimated by volumetric calculations using existing geological, geophysical and well data. The criteria used are described and the sensitivity of the results discussed.

The longevity of the field is studied using a two-phase numerical simulator (SHAFT79). A number of cases are studied based upon different boundary conditions, and injection and production criteria. Constant or variable mass production is employed in the simulations with closed, semi-infinite or infinite reservoir boundaries. In one of the cases, a fault zone feeding the production region is modeled. The injection strategy depends on the available waste water. The results of these simulations are discussed and the sensitivity of the results, with respect to mesh size and the relative permeability curves used, are briefly studied.

INTRODUCTION

The Baca geothermal field is located in the Valles Caldera, New Mexico, about 55 miles north of Albuquerque. The field is being developed by the Union Oil Company of California and the Public Service Company of New Mexico. To date, over 20 geothermal wells have been drilled in the Valles Caldera, varying in depth from 2000 to over 9000 feet (1). Six of the wells have been drilled in the Sulfur Creek area, the remainder along Redondo Creek (Fig. 1).

The wells in the Sulfur Creek area have penetrated a high-temperature but low-productivity formation. In the Redondo Creek area, the wells have encountered a high-temperature ($\geq 550^{o}F$) liquid-dominated reservoir. Interpretation of the well data by Union Oil (1) indicates the presence of a liquid dominated reservoir and a separate steam reservoir, which are not in hydraulic communication. However, a recent study by Grant (2) suggests that there is actually only one liquid-dominated reservoir, with an overlying two-phase zone.

It is extremely important to make reliable estimates of the mass of hot water in place (reservoir capacity) and the length of time the reservoir can supply steam for a 50 MW power plant (reservoir longevity). The reservoir longevity depends both on the reservoir capacity and on the overall development plan for the field (flow rates, injection, etc.) This paper represents the first in a series of studies of the reservoir capacity and longevity of the Baca field.

In this first study the reservoir capacity is estimated by volumetric calculations, using existing geological, well, and geophysical data. An initial study of the reservoir longevity is also made using the two-phase numerical simulator SHAFT79, developed at LBL. Because of the lack of available data, we made a number of assumptions during the course of the study. Therefore, the results presented here are preliminary. New estimates will be made as more data are accumulated.

GEOLOGY

The topographically high Valles Caldera is a subcircular volcanic depression, 12 to 15 miles in diameter, formed 1.1 million years ago. This resurgent caldera is characterized by a ring fracture zone where a number of rhyolitic volcanic domes are found (1). A broad structural dome, with a summit at Redondo Peak, is located near the center of the caldera and is bisected by a large northeast trending central graben (Redondo Creek). A detailed geological description of the Valles Caldera region can be found in references 3, 4 and 5. Geologic cross-sections of the Valles Caldera region are shown in Figure 2.

References and illustrations at end of paper.

The Bandelier Tuff is composed of several members of closely welded to non-welded rhyolitic tuff and tuff breccia (3). Up to 6300 feet of the tuff have been penetrated by the wells in Redondo Creek. The matrix permeability of the tuff is generally low, but open fractures provide permeable channels in its deeper layers. The bulk of the produced water in the existing commercial wells comes from the Bandelier Tuff (1).

The Paliza Canyon Andesite underlies the Bandelier Tuff and varies in thickness from 0 to over 2000 feet. It is believed to have low permeability due to its low matrix permeability and the lack of open fractures (1).

Some of the wells in Valles Caldera have penetrated a thin layer of poorly consolidated Tertiary sands and deeper layers of sedimentary rocks (Abo Formation). These overlie the basement rock in the Valles Caldera region, a Precambrian granite.

RESERVOIR CAPACITY

Previous Work

Union Oil (1) has estimated the "minimum" reservoir capacity of the Baca field by two independent methods; using a depletion equation, and interference test data. The depletion equation is a simple mass balance equation that has been successfully used in the oil and gas industry. This approach generally requires the reservoir to be fully confined (i.e., no natural recharge), and to contain a single phase fluid. The method does not consider temperature variations within the reservoir; i.e., only the mass of fluid in place is estimated. Using the depletion equation, Union Oil estimated the "minimum" reservoir capacity to be $\underline{4.74 \times 10^{12}\text{ lbs of fluid}}$.

An interference test was performed in the Baca field from October 1975 to April 1976 (1). Three wells were used for production, three for injection, and four for observation. Only one of the observation wells showed a distinct pressure response during the test, and only data from this well were used to estimate the reservoir capacity. Using superposition of the Theis solutions, the best match with the data was obtained when all active wells (production and injection) were considered and the reservoir was assumed to be infinite. With this information the areal extent of the reservoir was calculated to be at least $\underline{43\text{ mi}^2}$ and the "minimum" reservoir capacity to be $\underline{4.69 \times 10^{12}\text{ lbs of fluid}}$. This method also calculates the total mass of fluid in place (without considering the temperature of the fluid) and assumes that the reservoir contains only liquid water.

Volumetric Estimation

As a first step, we have made a volumetric estimation of the hot water contained in the reservoir (reservoir capacity). The parameters needed to calculate the reservoir capacity are the areal extent of the hot water zone and the average thickness and porosity of the reservoir. Geological information, well data, and shallow thermal-gradient contours were used to estimate the areal extent of the hot water zone. These data are supported by geophysical data from telluric and magnetotelluric (MT) surveys performed by Geonomics in 1976 (6), and a controlled-source electromagnetic (EM) survey performed by Group 7 in 1972 (7). Telluric data can give information regarding lateral variations in resistivity while magnetotelluric and electromagnetic soundings are mainly sensitive to resistivity variations with depth. The telluric and magnetotelluric lines are shown in Figure 1; the electromagnetic sounding points are not shown but they form a discrete series of measurements through Redondo and Jaramillo creeks.

The reservoir temperature contours are coarse and not very reliable due to the limited amount of available data. The contours indicate, however, a sharp temperature gradient southeast of the main temperature anomaly (Fig. 3). The shallow temperature gradient contour map (Fig. 1) shows a similar sharp decrease in temperature to the east.

These gradients probably result from either the presence of a permeability barrier between Redondo Creek and Redondo Peak or an inflow of colder water from the southeast into the hotter reservoir. The mapped fault between Redondo Creek and Redondo Peak (3) detected by telluric profile G-G′ (Fig. 1) tends to support the former explanation. We therefore deduce that the hot reservoir boundary to the east lies between Redondo Creek and Redondo Peak.

The shallow temperature gradients and geophysical data were used to estimate the hot reservoir boundaries in the north-south direction. The deep reservoir contour map is too localized to give this information. Figure 4 shows the shallow temperature gradients and the telluric profiles along line B-B′. The telluric data indicate a resistivity low extending from station 12 to station 28 or 29, which corresponds well to the area of high thermal gradients. The higher frequency plots do not show this anomaly, suggesting that the conductor lies deep (the lower frequency signal penetrates deeper). Magnetotelluric data also show a resistivity low over the same area and a layered resistivity model fit to the data indicates a conductor (5-20 ohm-m) at an approximate depth of 1 km (7). We will assume that the resistivity anomaly is due to the presence of the hot reservoir and that the boundaries of the hot reservoir correspond to stations 12 and 29 in the south and the north, respectively.

To the west, the temperature data are too limited to help establish the hot water reservoir boundary. The telluric profiles along lines D-D′ and H-H′ together with magnetotelluric data do, however, show a distinct resistivity contrast near the Bond-1 well; the low resistivity anomaly extends to the east. As the Sulfur Creek wells are hot but not productive, the resistivity anomaly seems to reflect formation porosity variations. Due to the lack of additional data to support this possibility we will assume that the reservoir extends as far west as the primary reservoir formation, the Bandelier Tuff. This assumption places the western limit of the reservoir at the ring fracture zone. By the above criteria, the estimated areal extent of the hot reservoir is approximately $\underline{40\text{ km}^2}$ (Fig. 1).

The average thickness of the reservoir was estimated using the well temperature logs and geological data. The base of the caprock was estimated from the temperature logs as the depth at which convection starts to control the heat transfers (i.e., the depth where the temperature gradient becomes small). The bottom of the reservoir was assumed to correspond to the bottom of the Bandelier Tuff (Fig. 2), yielding an average reservoir thickness of 2000 feet.

Few data are available regarding the matrix porosity of the Bandelier Tuff. After studying well resistivity logs and core data (8), we assumed an average porosity of 5%. The product of the porosity and the thickness (ϕH) is then 100 ft, corresponding very closely to the value of 90 ft obtained from the interference test in the Redondo Creek area (1).

The estimated reservoir capacity can be calculated as a product of the areal extent of the hot reservoir and its average porosity-thickness product. Using a density of 825 kg/m^3 (for a temperature of 450°F) the reservoir capacity is 2.2 x 10^{12} lbs of hot fluid.

Sensitivity of Results

In the estimation of the reservoir capacity a number of assumptions were employed. Some of the more important ones are listed below.

1. The reservoir contains liquid water only.
2. The hot fluid reservoir extends to the northwest as far as the ring fracture zone.
3. The subsurface resistivity low is due to the presence of the hot water reservoir.
4. The reservoir resides in the lower part of the Bandelier Tuff and does not extend into deeper formations.

If a two-phase zone overlies the main liquid water reservoir, the first assumption could lead to overestimation of the reservoir capacity. Similarly, if the reservoir does not extend all the way to the ring fracture zone, as the dry wells in Sulphur Creek might indicate, the reservoir capacity might again be overestimated. If, on the other hand, the production reservoir is fed by a deeper source of hot water, the estimated value of the reservoir capacity may be too conservative.

RESERVOIR LONGEVITY

Previous Work

Union Oil (1) has estimated the potential generating capacity of the Baca field. In their study, Union assumed the reservoir to be closed, the separator steam fraction to be constant (34%), and the amortization period to be 30 years. Furthermore, Union Oil assumed that all of the fluid in place was hot and could be extracted from the reservoir. When the no-injection case was considered, the generating capacity was estimated to be 410 MW. Using injection, and assuming that the original fluid in place is recycled three times, the calculated generating capacity was 939 MW and 1246 MW for an average reservoir porosity of 18% and 5%, respectively.

Numerical Approach

The longevity of the Baca field was studied using the two-phase simulator SHAFT79. A brief description of the computer code is given in the next section. The reservoir was simulated using a basic rectangular mesh, with overall dimensions corresponding to those estimated in the previous section (Fig. 5). Due to symmetry, we only modeled half of the system. Rather than simulating individual wells, the fluid was produced uniformly over one node representing half of the well field (assumed to be 1 km^2).

The parameters used in the simulation are given in Table 1. Most of these parameter values were taken directly from open-file Union reports. For the permeability-thickness product (kH), the value (6000 md·ft) obtained from the interference test performed by Union Oil (October 1975 to April 1976) was used. This value compares favorably with well test data from individual wells. The porosity-thickness product we used was the value estimated in the previous section (100 ft).

In the simulations a version of Corey's relative permeability equations was used (10). Mathematical expressions for Corey's 4th order equations are given in Table 3. The residual liquid and steam saturations were fixed at 0.30 and 0.05, respectively. In order to study the effects of the relative permeability curves on the results, various other curves were used. The findings of this study are discussed in a later section.

Computer Code Used

The numerical simulator SHAFT79 solves the mass and energy transport equations for two-phase flow in porous media. It employs the integrated finite difference method (IFDM) which allows simulations of complex geological features in one-, two-, or three-dimensions (11). The mass and the energy transport equations are solved simultaneously using the Newton/Raphson iterative procedure. The linear equations that arise at each iteration are solved with an efficient sparse solver (12).

The primary assumptions employed in SHAFT79 are as follows (13):

1. The flow of steam and water can be described by Darcy's law, with the interaction between the two phases represented by relative permeability functions.
2. The liquid, vapor and rock matrix are in local thermodynamic equilibrium.
3. The effects of capillary pressure are negligible.

The numerical code has been extensively validated against available analytical and numerical solutions for single- and two-phase flow through porous media. A detailed description of the simulator is given by Pruess and Schroeder (13).

Simulations Using a Constant Mass Flowrate

We studied five cases using a constant mass flow rate. The value we used was based upon the amount of steam theoretically required for a 50 MW power plant and a constant value of the mass fraction of steam in the separators (1). The five cases studied were a bounded reservoir, an infinite reservoir, and three injection cases. Each case was run until the pressure in the production node dropped below the designed well head pressure of 10 bars (1). The longevity of the field in each case was defined as the time it took to reach this point. The pressure, temperature, and vapor saturation at the production node are plotted versus time for three of these cases (Fig. 6).

The simulation of the closed reservoir was terminated after 7.4 years due to the low pressure in the production node. As Figure 6 shows, the pressure falls very rapidly until the production node goes two-phase. Under two-phase conditions, the pressure is not related to the density but to the temperature. The pressure first stabilizes after the node becomes two-phase because of the the large heat capacity of the node and the low initial boiling rates. Later the pressure gradually declines along with the temperature. When the vapor saturation reaches 1.0, the pressure again becomes dependent on density, and the low inflow of fluid from adjacent nodes (due to the low absolute permeability and the effect of the relative permeability curves) causes the pressure to drop very rapidly.

Figure 7 shows the variation with time of the boiling rate at the production node, the vapor saturation of the produced fluids, and the vapor saturation in the adjacent nodes for the bounded reservoir case. The boiling rate increases rapidly soon after the production node becomes two-phase and reaches a maximum when only steam is produced. At that time the boiling rate corresponds to the production rate. Later, the boiling rate decreases again due to the decreasing mass of fluid entering the production region. The increasing vapor saturation in the nodes adjacent to the production node causes a reduction in the mobility of the liquid phase and consequently decreases the mass of fluid entering the production node.

For the infinite reservoir case a larger mesh (20 x 21 km^2) was used. The results indicate that the pressure in the production region will drop below 10 bars after about 10 years, again due to the limited flow of fluids into the production node (low permeability effects). The general behavior of the temperature, pressure, and vapor saturation is the same as for the bounded reservoir case (see Fig. 6). This shows that the factor controlling the longevity appears to be the low permeability-thickness product rather than the amount of hot water in place.

Three injection cases were simulated using an injection flow rate equal to half the production mass flow rate. The reservoir boundaries were closed. The water was injected 1 km to the southeast (node 21), 1 km to the northwest (node 19), and 4 km to the northwest (node 16) of the production region for the three cases. In each case the pressure in the production node dropped below 10 bars after 13 to 14 years.

Figure 6 also includes a plot of the temperature, pressure, and vapor saturation versus time in the production node when water is injected through node 21. The curves are similar to those for the no-injection case, except that the pressure falls below 10 bars before the production node reaches superheated steam conditions. This behavior is due to increased boiling in the production node since more water is coming in. The boiling causes the temperature, and consequently the pressure, to drop steadily. The other two injection cases show similar behavior. Table 2 summarizes the results for the five cases.

Simulations Using a Variable Flow Rate

Generally during a simulation, the vapor saturation in the production node constantly changes, and consequently the steam quality in the separators changes. For a given power production a certain mass of steam is needed, and the amount of fluid mixture from the reservoir should be adjusted to meet that requirement. The assumption of a constant mass flow rate, which was used in the simulation described above, is therefore inaccurate and leads to lower estimates of reservoir longevity.

In order to calculate the flow rates as a function of steam quality in the separators, the simulator SHAFT79 had to be modified slightly. Assuming isoenthalpic conditions, i.e., the fluid loses no energy on its way up the well and into the separators, the steam quality (S_q) can be simply calculated as follows:

$$H_w = (1 - S_q)\, H_{sl} + S_q\, H_{sv} \qquad (1)$$

In this equation, the enthalpy of the fluid entering the well (H_w) is not the same as the enthalpy of the production node, because the fluid is produced according to the relative permeabilities of the individual phases.

The theoretical steam requirement for a 50 MW plant (Q_s) is 892,000 lbs/hr (1), so that the required total flow rate (Q_t) can be calculated at any time as:

$$Q_t = Q_s/S_q \qquad (2)$$

Four cases were simulated using a variable flow rate; a closed reservoir, a semi-closed reservoir, an infinite reservoir, and a closed reservoir with recharge from deeper layers. In the semi-closed case, the northeast and the southwest boundaries were expanded from 3 to 10 km, leaving the other two boundaries unchanged. No injection runs were made, because very little separated water was obtained after about three years of simulation, and injecting such a small amount of water would not alter the results significantly. Figure 8 shows the calculated flow rate as a function of time for the bounded reservoir case.

The closed reservoir case and the semi-closed reservoir case gave very similar results; the pressure in the production node dropped below 10 bars after 25 and 26 years, respectively. In the "infinite reservoir" case the same large mesh was used (20 x 21 km^2), and the required amount of steam was supplied for 35 years before the pressure fell below 10 bars.

Finally, a run was made assuming that the reservoir was recharged from deeper layers through a 20 m wide fault zone extending along Redondo Creek (recharging nodes 6, 13, and 20). The fault zone was modeled as a constant pressure boundary 600 m below the assumed reservoir, having a permeability-thickness product of 60,000 md·ft. The results obtained indicate a reservoir longevity of 49 years under these conditions. The variable flow rate cases are summarized in Table 2.

Sensitivity of Results: Mesh dependence and effects of relative permeability curves.

In modeling two phase flow in geothermal reservoirs, one must consider two important factors: the mesh dependence of the results, and how dependent the results are upon the particular relative permeability curves used. We conducted a brief study to determine the sensitivity of our results to these factors.

In order to determine the sensitivity of the results to the mesh used in the simulations, a new, finer mesh was constructed. The fine mesh consists of 81 elements, each element having a volume four times smaller than the corresponding element used in the earlier simulations (Fig. 5). The production element, however, remained the same size. Using the fine mesh we studied the case of a constant mass flow rate with closed reservoir boundaries (case #1). Figure 9 shows a comparison between the fine and the coarse mesh results for the pressure behavior in the production node. Although the two curves are quite similar at early times, the curve corresponding to the fine mesh is shifted about 2 bars above the curve corresponding to the coarse mesh.

This behavior can be explained if one considers that in the case of the fine mesh, the nodes adjacent to the production node undergo phase transition (to a two-phase condition) at an earlier time than the larger nodes in the coarse mesh, and consequently steam flows into the production node at an earlier time. This in turn implies that less boiling will be required in the production node in the case of the fine mesh at any given time, resulting in a smaller pressure drop. However, the higher steam flow into the production node in the fine mesh case causes higher vapor saturation at any given time in the node, so that superheated conditions are reached earlier. It is therefore apparent that in terms of longevity, the coarser mesh gives results that are slightly more optimistic (increased longevity) than what can be expected.

In our study of the effects of the relative permeability curves on our results, we used curves suggested by Counsil and Ramey (14) and Grant (15) in addition to the Corey curves. The curves by Counsil and Ramey are based upon experimental results over a small range of vapor saturation (.20 < S < .30), and for our simulation studies the data was linearly extrapolated to cover the full range of saturation. The curves developed by Grant (15) are based upon data from the Wairakei geothermal field. The relative permeability of the liquid is the same as given by the 4th order Corey equations, but the steam phase is considerably more mobile. Mathematical expressions for the curves used in this study are given in Table 3, and the curves are illustrated in Figure 10.

Figure 11 shows pressure behavior at the production node for case #1 and different relative permeability curves. The figure shows that the longevity (the time when the pressure falls below 10 bars) is basically unaffected by the particular relative permeability curve chosen. The pressure plots based on the Counsil and Ramey curves lie at all times below the results based upon Coreys equations. This is to be expected since the mobilities of the steam and the liquid are generally less in the case of the Counsil and Ramey curves. The pressure behavior based on Grant's curves is less at early times than in the case of Corey's curves, because more of the steam is being produced and consequently, more boiling occurs in the production node. One must keep in mind that the mass ratio of steam and liquid produced depends on the relative permeability curves used. However, in the case using Grant's curves, the longevity is slightly higher, because of the much more mobile steam phase.

In addition to the runs shown in Figure 11, a couple of runs were made using modifications of the curves by Counsil and Ramey. In the first run the steam was made immobile at a vapor saturation of 0.60, but the relative permeability of the steam increased linearly, becoming fully mobile at a vapor saturation of 1.0. The results obtained agreed very closely with the former run using Counsil and Ramey's curves, indicating that the steam relative permeability curve may not be very important for this problem.

In the second case studied, the residual water saturations were fixed at 0.60, and the curves were again linearly extrapolated to become fully mobile at a vapor saturation of 0.0. In this case the longevity increased to almost 9 years. The increased mobility of the water phase causes considerably more liquid to enter the production node and consequently the longevity increases.

A brief study was made of the effects of the relative permeability curves on the longevity when a variable mass flow rate is used. In the study the curves of Counsil and Ramey were used and the results compared to those obtained when the Corey curves were used. The results compared quite well and a longevity of 23 years was obtained for the former case, compared to 25 years for the latter (case #6).

CONCLUSIONS

We have estimated the reservoir capacity and the longevity of the Baca field using a volumetric approach and the numerical simulator SHAFT79. The areal extent of the hot reservoir was estimated to be 40 km^2 and the porosity-thickness product to be 100 feet. These values correspond to a reservoir capacity of 2.2×10^{12} lbs of hot fluid in place.

We also studied the longevity of the Baca field, using either constant or time-dependent production rates. Five cases were studied using the constant rate: one closed reservoir, one infinite reservoir, and three injection cases. All of these cases showed that the flow rate could be maintained no longer than 15 years due to the resulting low pressure in the production region. In a low-permeability reservoir which the Baca reservoir appears to be, the boiling is very localized, causing a rapid drop in the temperature and, subsequently, in the pressure in the production region. The constant flow rate cases represent an overly pessimistic situation, because the steam quality of the produced fluids increases with time, and consequently a smaller total amount of fluid is actually needed for a 50 MW power plant.

For the cases of variable production the flow rates are calculated based on the steam required for a 50 MW power plant and the steam fraction in the separators. These runs indicate a reservoir life of 25 to 49 years, depending upon the assumed reservoir boundary conditions.

In studying the sensitivity of our longevity estimates, we have found that the results are mesh dependent to some degree and that the longevity values obtained by using the coarse mesh may be slightly optimistic. A brief study using relative permeability curves suggested by Counsil and Ramey and by Grant seems to indicate that the results are not very sensitive to the particular relative permeability curves chosen. The key factor is the mobility of the liquid phase. If relative permeability curves are employed where the liquid phase is more mobile than in the curves we have used, the longevity may increase considerably.

In general, the studies of the longevity of the Baca field seem to indicate the following:

1. The controlling factor in determining the longevity of the Baca reservoir is the kH product of the system. The low kH product (6000 md·ft) obtained from well tests at Baca drastically limits the longevity of the field (see Table 2). This indicates the urgent need to determine the kH product more accurately, perhaps using an injection test rather than drawdown tests.

2. Placing the production wells over as large an area as possible will help to obtain the required steam supply, without reducing the

pressure below a critical value.

3. Injecting the waste water should increase the lifetime of the field considerably, but the available waste water may become very limited shortly after power production starts.

During the course of the study we made a number of assumptions, and therefore the results should be considered as rough estimates. When additional data are acquired, the estimates will be updated using more sophisticated methods.

NOMENCLATURE

H = reservoir thickness - m

H_w = enthalpy of the fluid entering the well - J/kg

H_{sl} = enthalpy of saturated liquid in flash tank - J/kg

H_{sv} = enthalpy of saturated vapor in flash tank - J/kg

k = permeability - m^2

k_{rs} = relative permeability of steam phase

k_{rw} = relative permeability of water phase

ϕ = porosity

Q_t = total flow rate - kg/s

Q_s = theoretical steam requirement for a 50 MW geothermal power plant - kg/s

S = vapor saturation

S_q = steam quality in flash tank

S_{rs} = residual steam saturation

S_{rw} = residual water saturation

ACKNOWLEDGEMENTS

We would like to thank M. J. Lippmann, K. Pruess, and J. H. Howard of Lawrence Berkeley Laboratory for many valuable discussions, and A. Wilbur and M. MarQuis of the U.S. Department of Energy for their support during the course of the study.

This work was performed under the auspices of the U.S. Department of Energy, Division of Geothermal Energy, under Contract W-7405-ENG-48.

REFERENCES

1. Union Oil Company of California and Public Service Company of New Mexico, 1978, "Geothermal Demonstration Plant," Technical and Management Proposal to DOE.
2. Grant, M., 1979, "Interpretation of downhole measurements at Baca", Proc. 4th Workshop on Geothermal reservoir Engineering, Stanford University, Stanford, California.
3. Bailey, R.A., and R.L. Smith, 1978, "Volcanic geology of the Jemez Mountains, New Mexico." J.W. Hawley (ed.) in Circular 163, New Mexico Min. Mines, pp. 184-196.
4. Dondanville, R.F., 1971, "Hydrological geology of the Valles Caldera, New Mexico," Union Baca Project Report, 36 pp.
5. Slodowski, T.R., 1977, "Geological resume of the Valles Caldera," Union Baca Project Report, 11 pp.
6. Geonomics, Inc., 1976, "Magnetotelluric-telluric Profile Survey of the Valles Caldera Prospect," private geophysical study performed for Union Oil Company.
7. Group 7, 1972, "Additional electrical geophysical surveys of the Valles Caldera Area," private geophysical study performed for Union Oil Company.
8. Core Laboratories Inc., 1975, Special core analysis study of Baca No. 13 Well, private study for Union Oil Company.
9. Pruess, K., J.H. Zerzan, R.C. Schroeder and P.A. Witherspoon, 1979, "Description of the Three-Dimensional Two-Phase Simulator SHAFT78 for Use in Geothermal Reservoir Studies," paper presented at Petr. Eng. Meeting in Denver, Colorado, February 1-2, 1979.
10. Faust, C.R., and J.W. Mercer, 1979, "Geothermal Reservoir Simulation - Numerical Solution Techniques for Liquid and Vapor Dominated Hydrothermal Systems," Water Resources Research, v. 15, No. 1.
11. Edwards. A. L., 1972, "TRUMP: A computer Program for Transient and Steady State Temperature Distribution in Multidimensional Systems," Lawrence Livermore Laboratory, Report UCRL-14754, Rev. 3.
12. Duff, I.S., "Ma28--A Set of FORTRAN Subroutines for Sparse Unsymmetric Linear Equations", Report AERE-R8730, Harwell/Oxfordshire Great Britain.
13. Pruess, K., and Schroeder, R., 1980, "SHAFT79--Users Manual" LBL Report LBL-10861, Lawrence Berkeley Laboratory, Berkeley.
14. Counsil, J.R., and Ramey, H.J., "Drainage Relative Permeabilities Obtained from Steam-Water Boiling Flow and External Gas Drive Experiments" Transactions, Geothermal Resources Council, vol. 3, September, 1979.
15. Grant, M.A., 1977, "Permeability Reduction Factors at Wairakei", paper 77-HT-52 presented at AICHE-ASME Heat Transfer Conference, Salt Lake City, Utah, August 15-17, 1977.

TABLE 1: PARAMETERS USED IN SIMULATION

Constant flow rate Q_t = 330 kg/s

Rock heat capacity C_v = 950 J/kg·°C

Perm. thickness kH = 6,000 md·ft

Thermal conduct. λ = 2.0 J/s·m·°C

Porosity thickness ϕH = 100 ft

Initial pressure P_i = 110 bars

Initial temperature T_i = 300°C

TABLE 2: SUMMARY OF CASES AND PRIMARY RESULTS

				Conditions at the end of the run			
Case	Flow rate	Boundary conditions	Injection	Time (yrs)	Pressure (bars)	Temp °C	Vapor saturation
1	Constant	Closed	None	7.4	10	237	1.0
2	Constant	"Infinite"	None	9.6	10	214	1.0
3	Constant	Closed	4 km to NW	12.9	10	180	0.99
4	Constant	Closed	1 km to NW	13.7	10	180	0.91
5	Constant	Closed	1 km to NE	14.0	10	180	0.87
6	Variable	Closed	None	25	10	214	1.0
7	Variable	"Semi-infinite"	None	26	10	213	1.0
8	Variable	"Infinite"	None	35	10	185	1.0
9	Variable	Bounded with a fault	None	50	10	180	0.48

TABLE 3: Relative Permeability Equations
(Plots are shown in Fig. 10).

1. Corey's Curves:

$$k_{rw} = \begin{cases} [S*]^4 & S < S_{rw} \\ 0 & S \geq S_{rw} \end{cases}$$

$$k_{rs} = \begin{cases} [1-S*]^2 \; [1-(S*)^2] & S > S_{rs} \\ 0 & S \leq S_{rs} \end{cases}$$

$$\text{where } S* = \frac{1 - S_{rw} - S}{1 - S_{rw} - S_{rs}}$$

2. Grant's Curves:

$$k_{re} = \begin{cases} [S*]^4 & S < S_{rw} \\ 0 & S \geq S_{rw} \end{cases}$$

$$k_{rs} = 1. - k_{rw}$$

3. Counsil and Ramey's Curves:

$$k_{rw} = \begin{cases} [1 - \frac{S}{.30}] & S < .30 \\ 0 & S \geq .30 \end{cases}$$

$$k_{rs} = \begin{cases} [\frac{S-.20}{.80}] & S > .20 \\ 0 & S \leq .20 \end{cases}$$

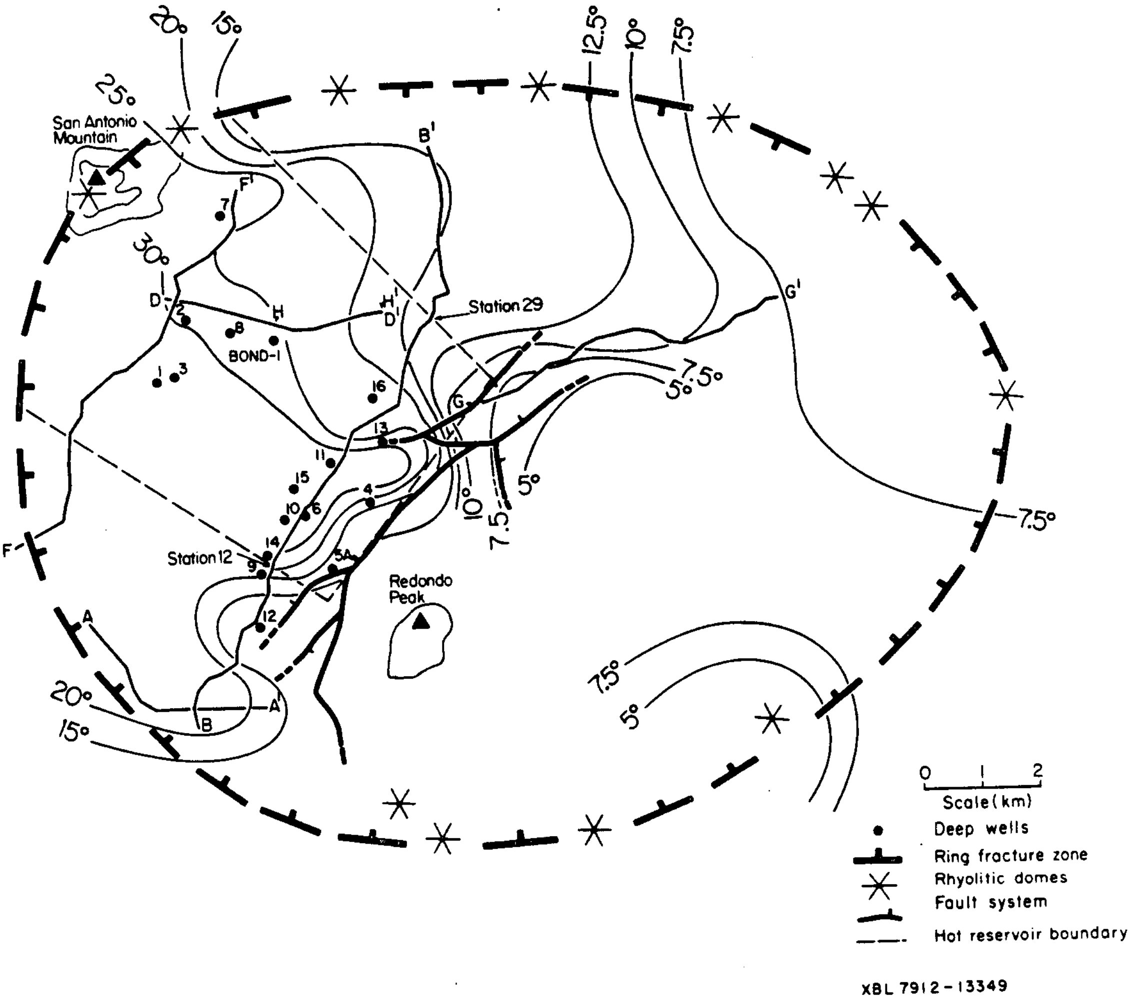

Fig. 1 Base map of the Valles Caldera showing shallow temperature gradients (^{o}F/100 ft.) geophysical survey lines (e.g., A-A'), specific faults, and the estimated hot reservoir boundary (ref. 1, 5 and 6).

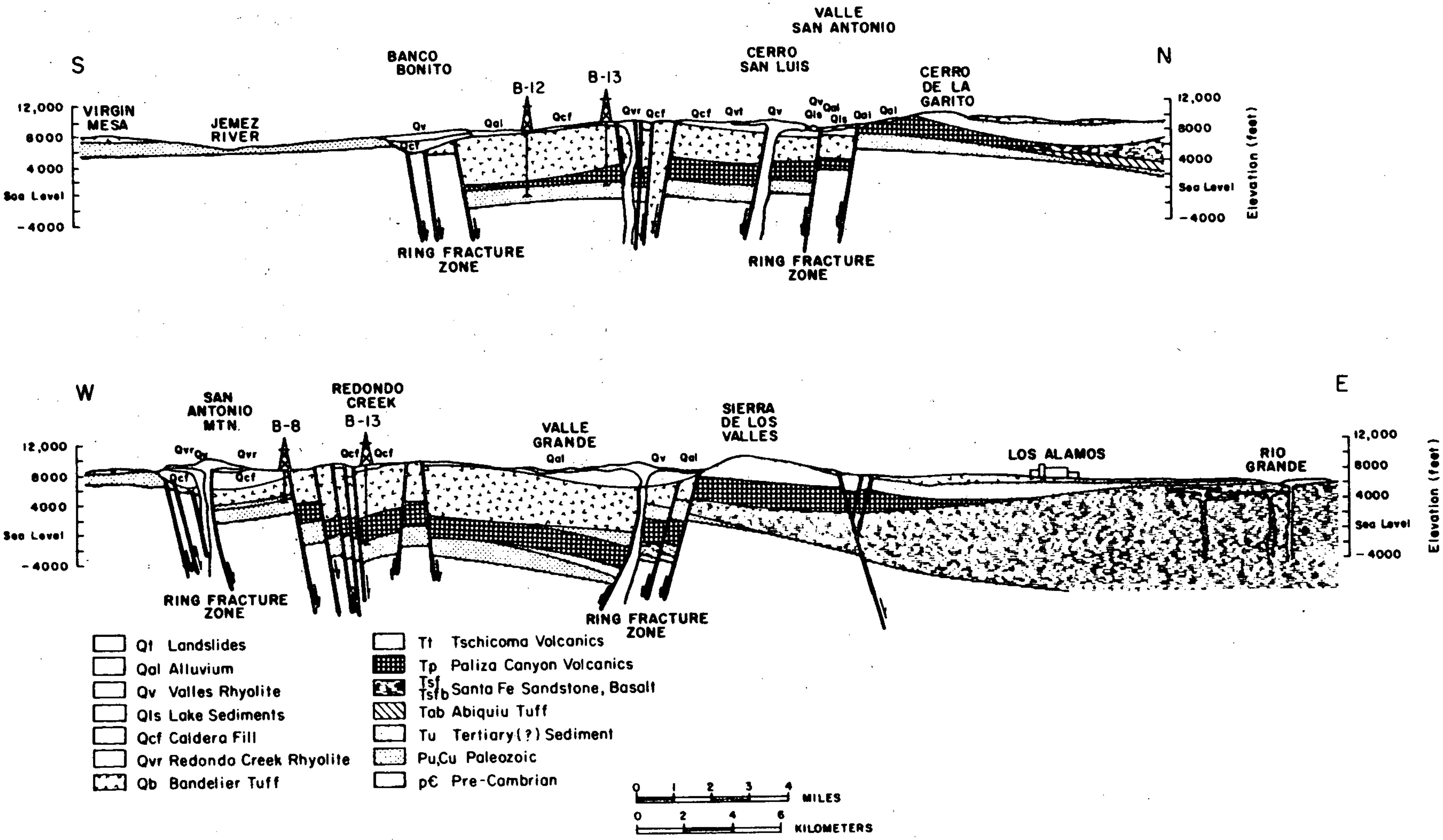

XBL 799-11548A

Fig. 2 Geologic cross sections of the Valles Caldera region.

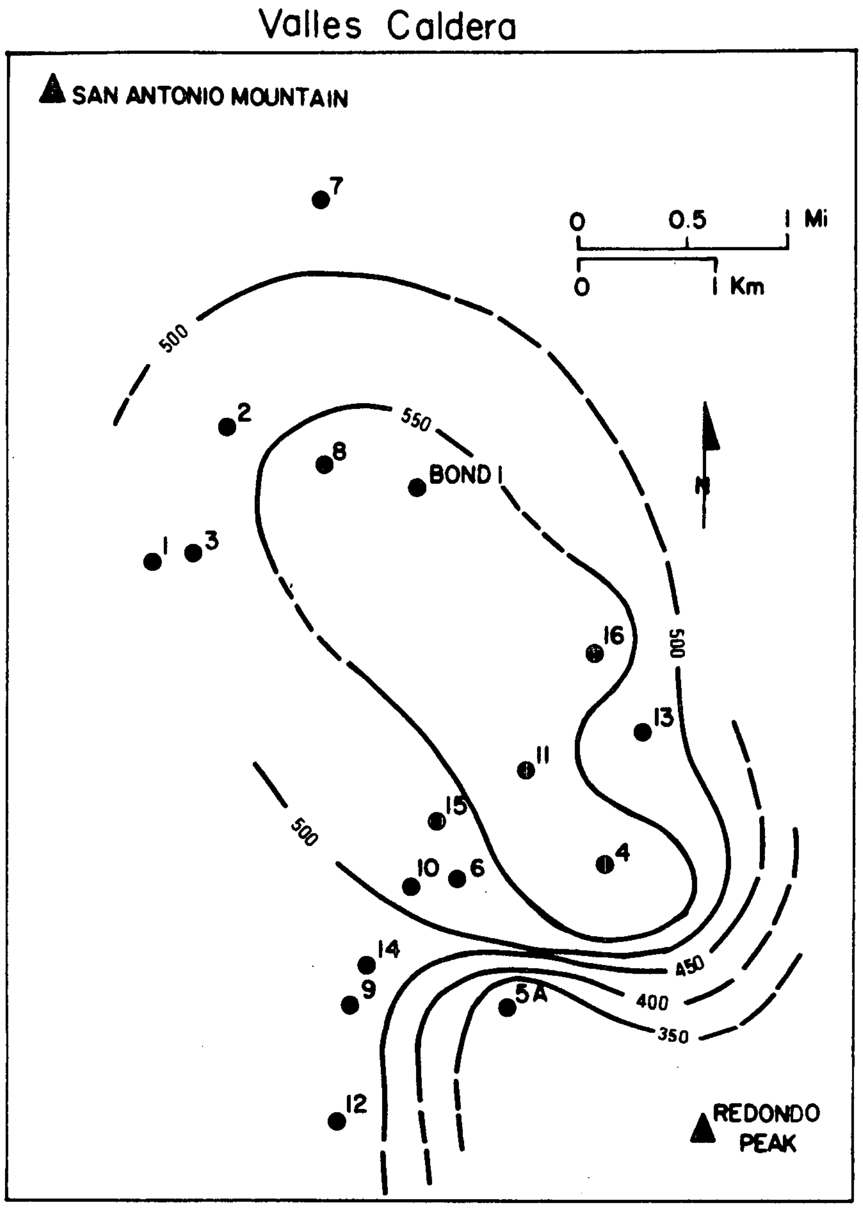

XBL 794-7414B

Fig. 3 Deep reservoir temperature contours (3000 ft. ASL) in °F.

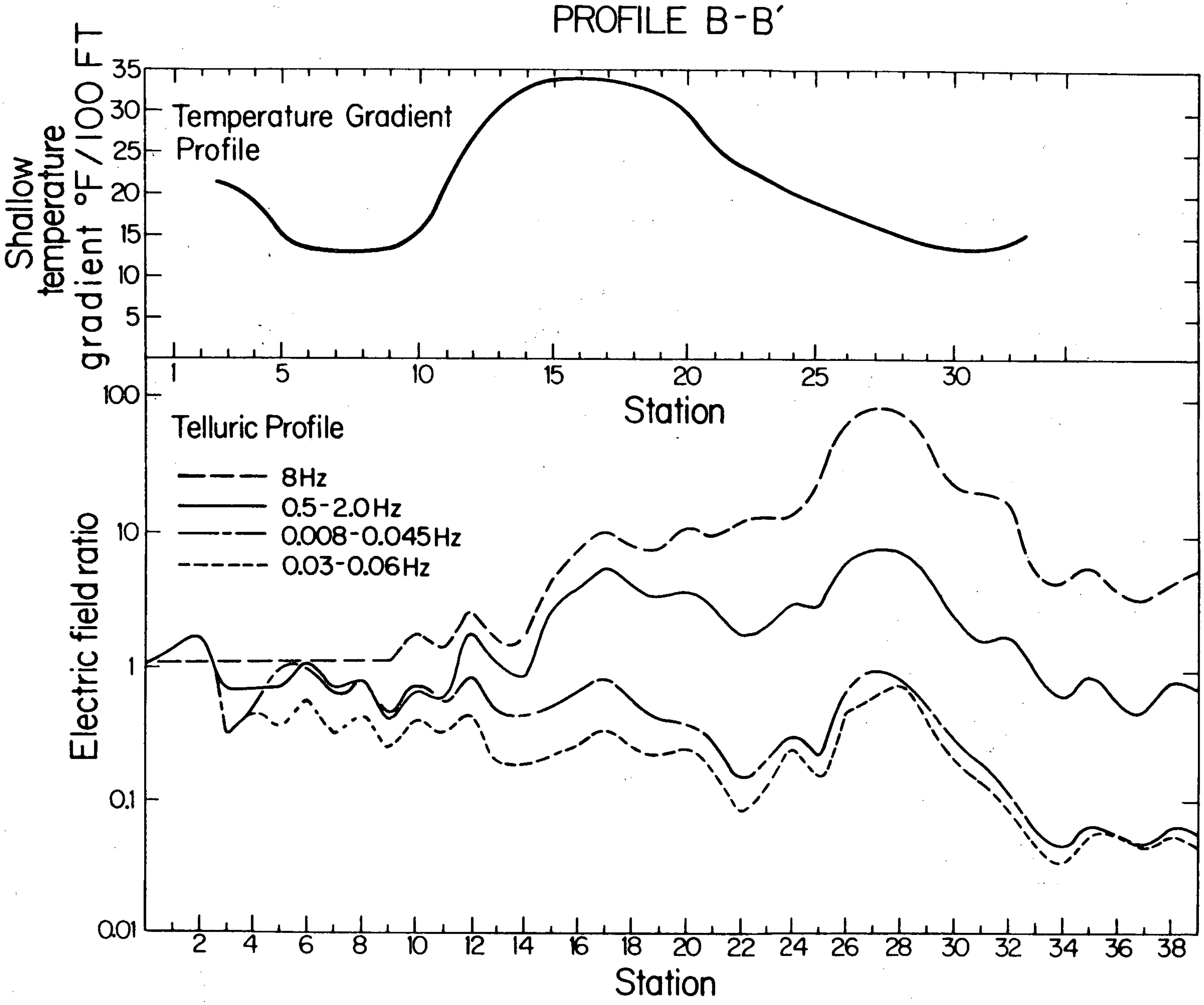

Fig. 4 Shallow temperature gradients and telluric profiles along survey line B-B'.

XBL 7912-13350

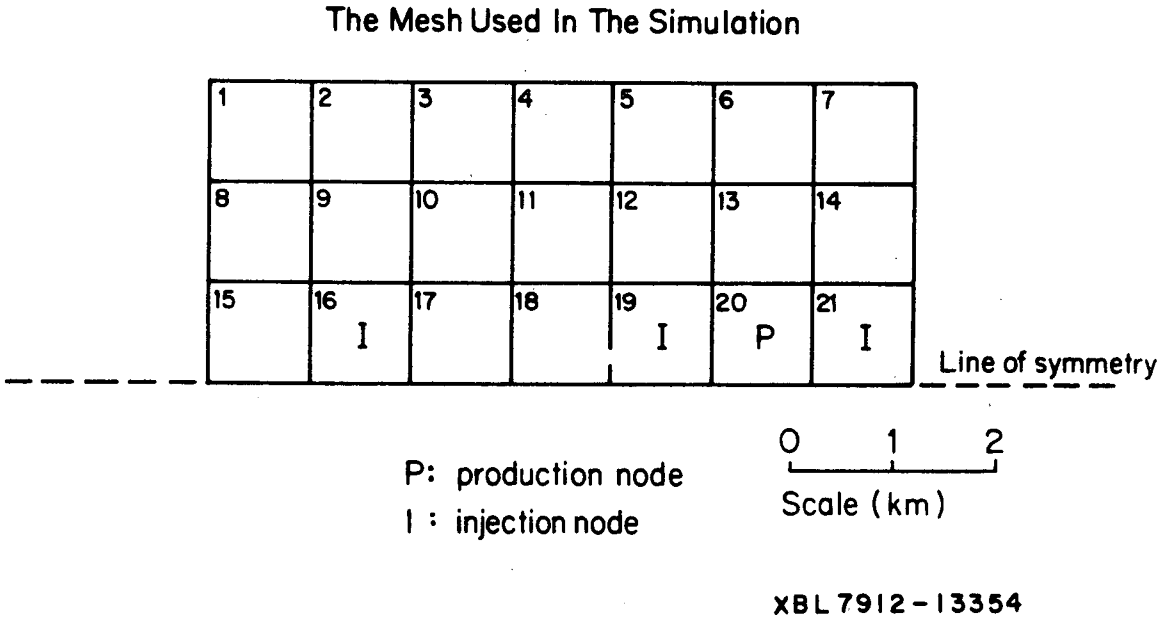

Fig. 5 The mesh used in the longevity study for "closed reservoir cases.

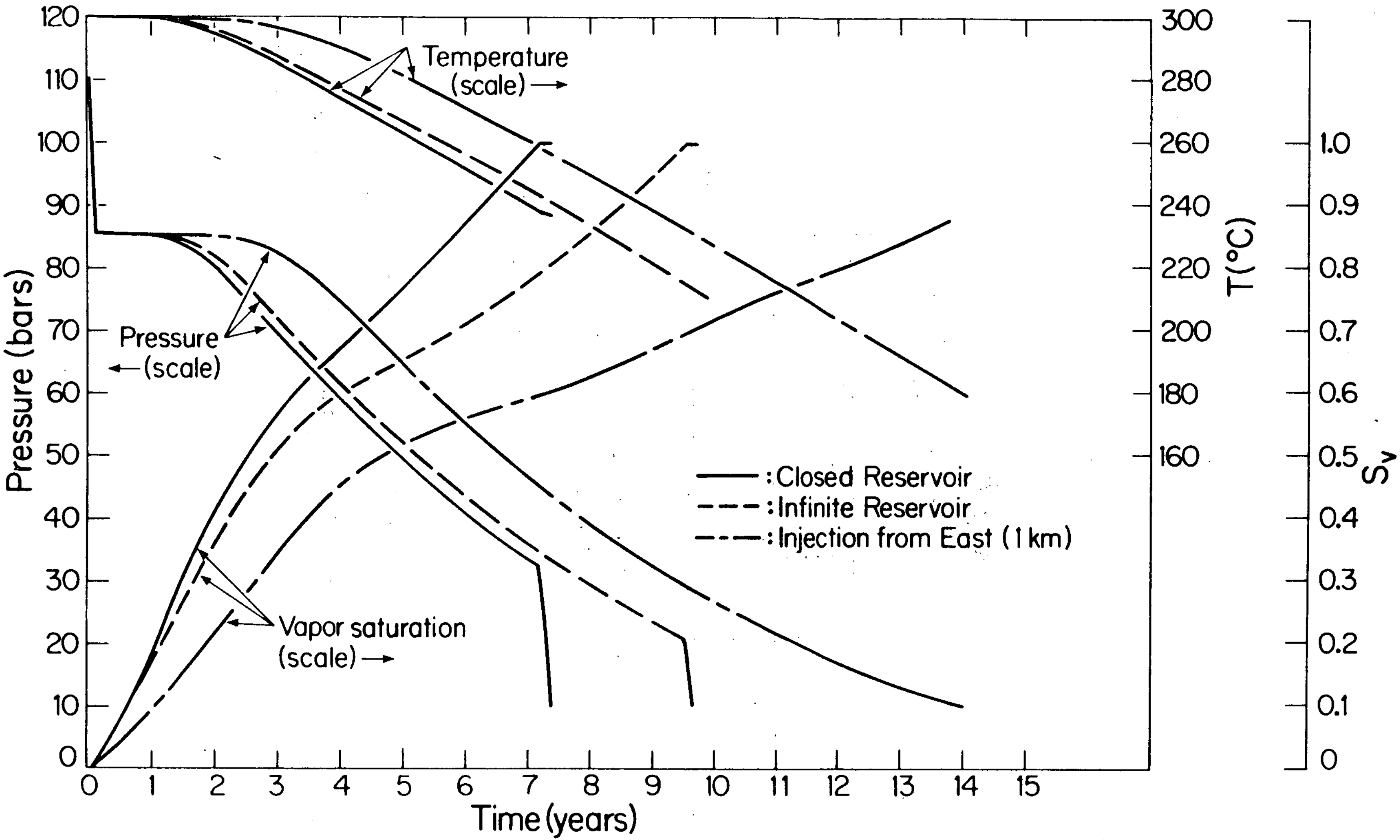

XBL 7912-13352

Fig. 6 The temperature, pressure and vapor saturation behavior in the production node for three of the constant flow rate cases.

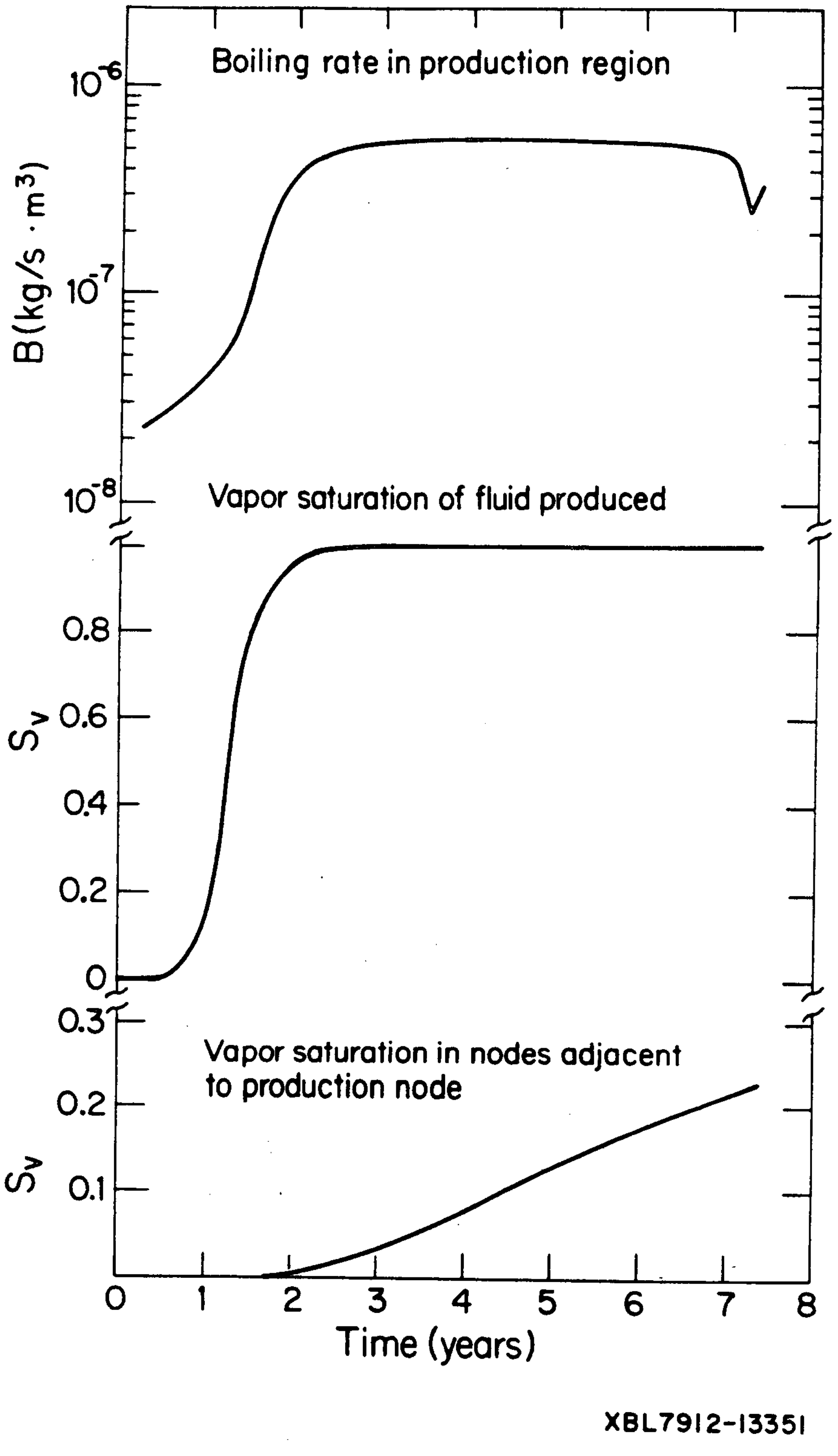

Fig. 7 Variation with time of boiling rates and vapor saturation for the constant production, closed boundary case.

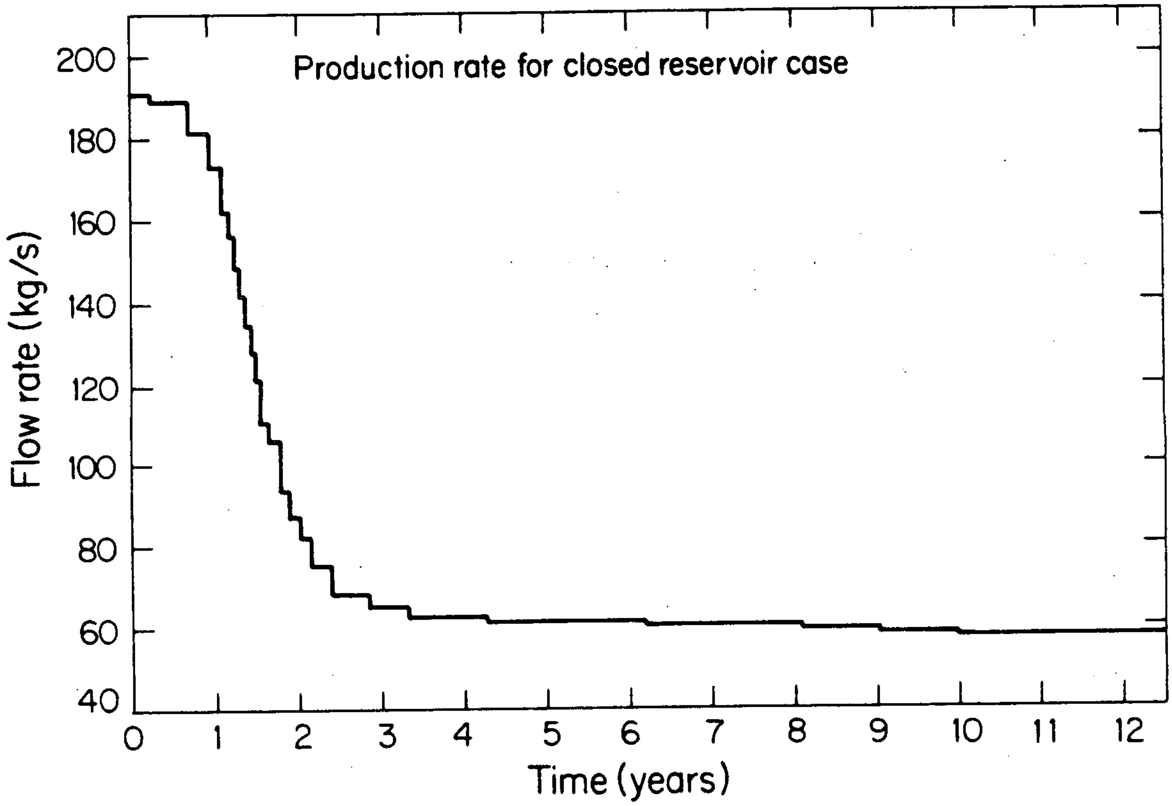

XBL7912-13353

Fig. 8 Production rate versus time for the closed boundary case.

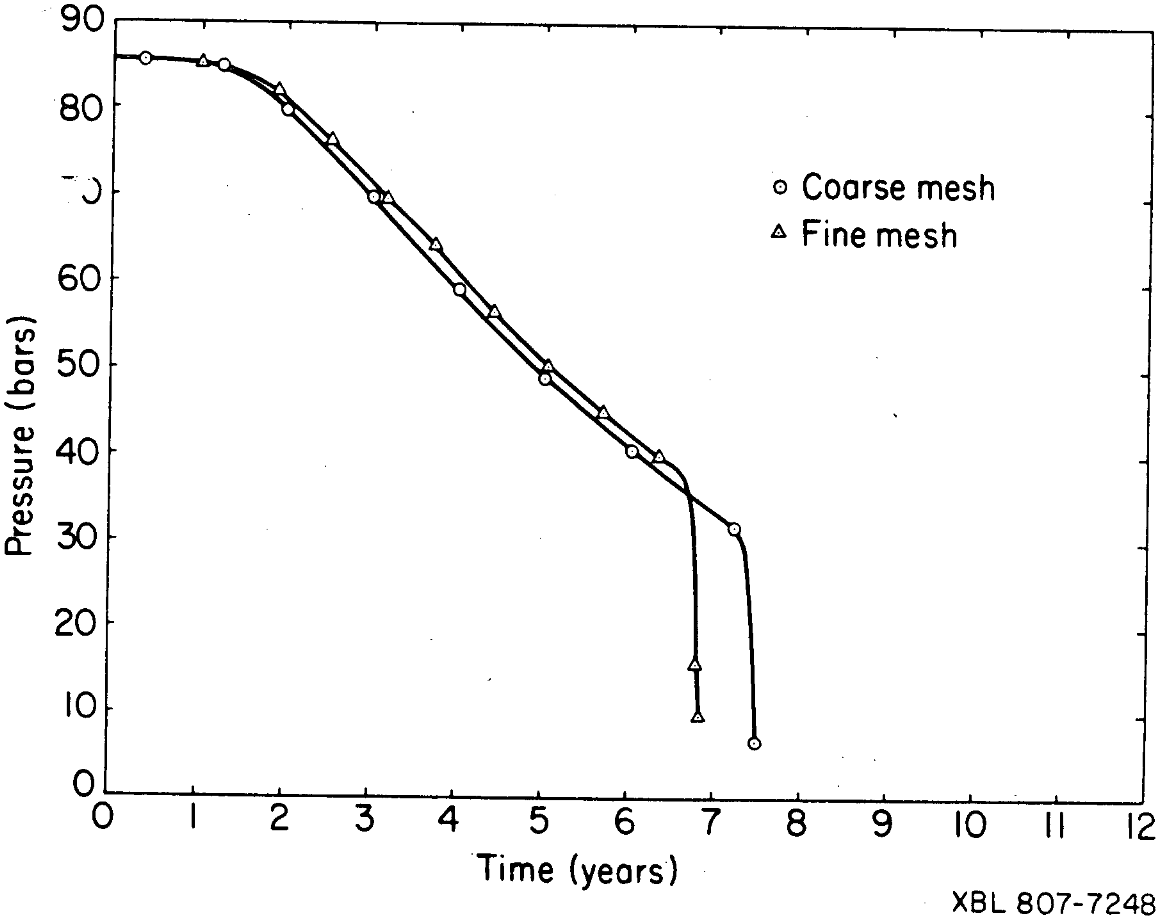

Fig. 9 **Mesh dependence: pressure behavior in production node.**

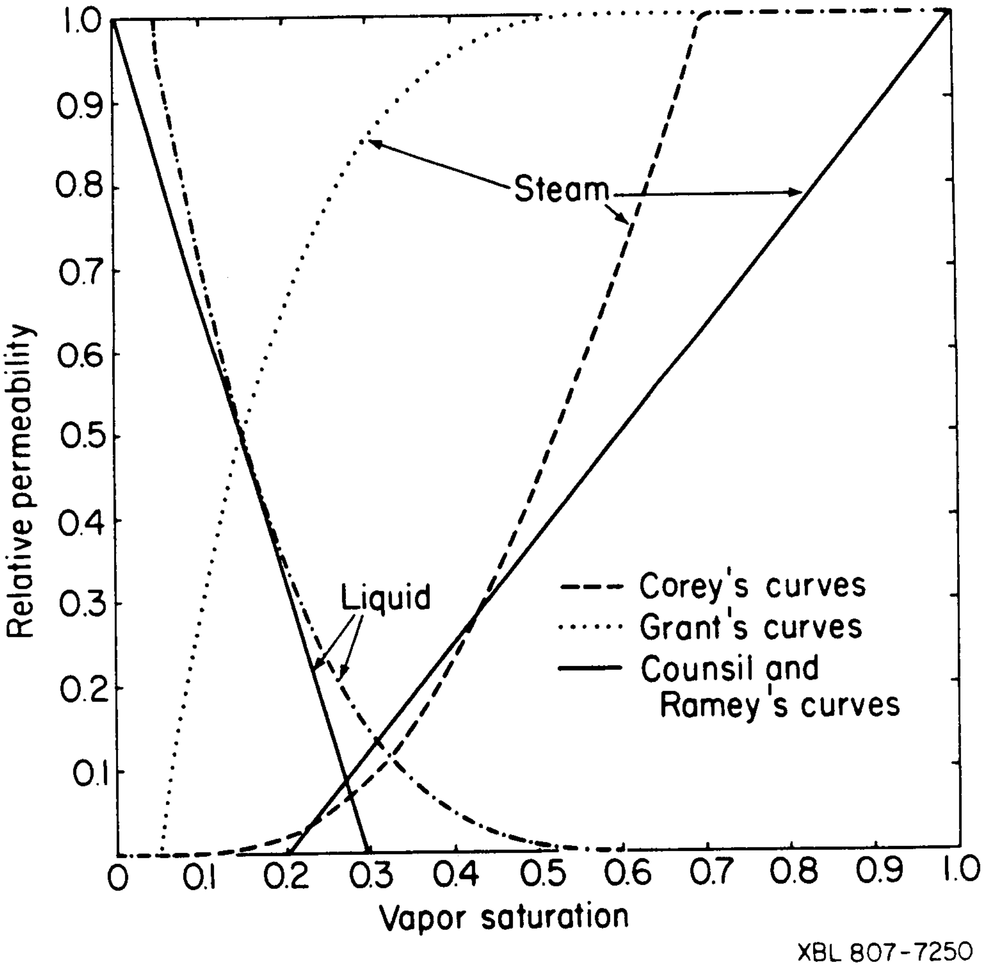

Fig. 10 Relative permeability curves used in the study.

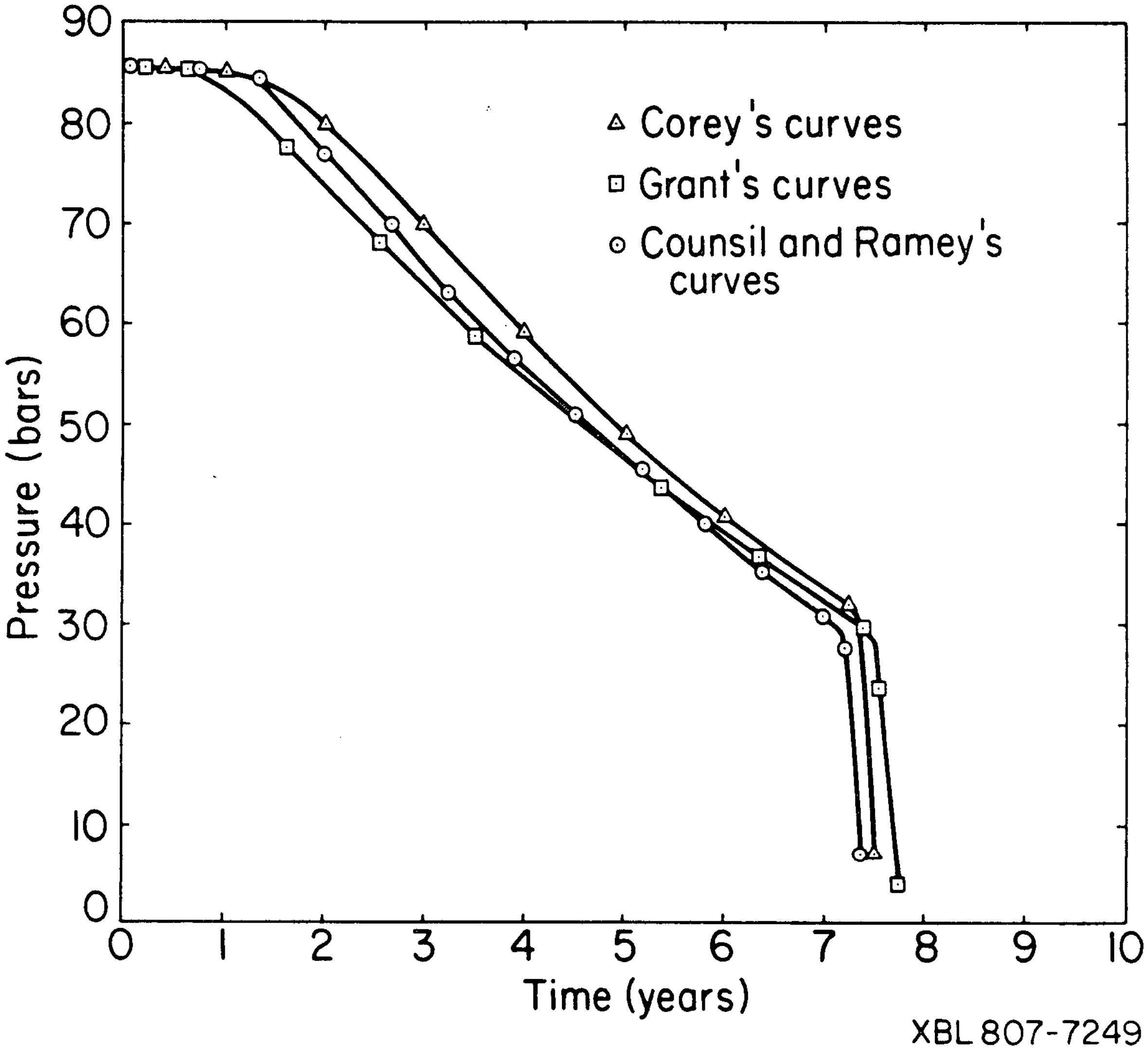

Fig. 11 Effects of relative permeability curves.

TECHNICAL INFORMATION DEPARTMENT
LAWRENCE BERKELEY LABORATORY
UNIVERSITY OF CALIFORNIA
BERKELEY, CALIFORNIA 94720